Application of the AWE Method with the 3-D TVFEM to Model Spectral Responses of Passive Microwave Components

Xiao-Ming Zhang and Jin-Fa Lee, *Member, IEEE*

***Abstract*— This paper describes an efficient algorithm to evaluate the spectral response of passive microwave devices. The method is based on the combination of the tangential-vector finite-element method (TVFEM) for modeling three-dimensional (3-D) microwave passive components and the asymptotic waveform evaluation (AWE) technique for efficiently computing the spectral responses. Unlike previous AWE approaches, which use direct matrix factorization to solve for the moments, we employ a preconditioned conjugate gradient (PCG) method. It is observed that the iterative PCG solver converges much faster by solving only the additional components of the higher moments outside the span of previous moments. Moreover, this paper discusses the effect of shifting the expansion frequency from the real frequency axis to the lower half of the complex frequency plane. Through several numerical examples, a waveguide with an obstacle inside, mitered 90° E- and H-plane waveguide bend, microstrip low-pass filter, and microstrip patch antenna, we show that shifting reduces the pollution due to dominant resonant modes and, consequently, results in a much wider convergence range for the moment-matching AWE technique.**

***Index Terms*— AWE, finite-element methods, microwave passive components, numerical methods.**

I. Introduction

SPECTRAL responses of electromagnetic (EM) devices are of great value for analysis and design purposes. Among various approaches for modeling microwave devices, the finite-element method (FEM), especially the tangential-vector finite-element method (TVFEM) [1], [2], has been demonstrated to be very successful. The TVFEM formulation of EM problems usually leads to a matrix equation with many unknowns. In order to obtain the system responses within the frequency range of interest, it is a common practice to solve the system equation directly at many frequencies. Subsequently, the results are interpolated to form a continuous curve. However, with the increasing size of the system, solving this system of equations at many discrete frequency points can be very time consuming. Especially when the system possesses a complex spectral behavior, with many resonances within the frequency range, it may be necessary to solve hundreds of solutions to obtain the desired resolution in the spectrum.

A number of model reduction techniques have been successfully developed for simulating transient responses in circuit analyses [3], [4], finding poles to determine the stability condition in feedback control process [5], and fast frequency-sweep techniques for EM devices modeling [6]. Among them, the asymptotic waveform evaluation (AWE) method [3] was originally developed for timing analysis of high-speed circuits. Through explicit moment matching, the AWE technique approximates the transient response of a circuit by reducing the problem to a low-order model. The poles of the reduced model are good approximations of the dominant poles of the original system. However, one major problem of the AWE technique is that it does not provide an accurate approximation (even with many moments) when the expansion point is very close to a pole (resonance of transfer function). More stable model reduction approaches (using variants of Krylov subspace methods) are proposed by Gallivan [5]. Furthermore, a Lanczos algorithm with an implicit restart process is proposed in [7], which ensures the reduced model always produces a stable approximation, and a rational Lanczos algorithm is presented in [8], which extracts information from multiple points and, therefore, provides improvements in the rate of convergence. These methods are usually very efficient and numerically stable. However, for Maxwell's equations, particularly with losses presented by lossy dispersive materials, as well as radiation boundary conditions, one has to extend the required Krylov subspaces to general matrix polynomials. In contrast, the explicit AWE can always be applied to realize a Padé approximation. The recently published complex frequency hopping (CFH) [9] technique for EM application is an AWE-based multipoint moment-matching method. It exploited a binary search scheme to match all dominant poles in a systematic manner. This CFH algorithm has been applied to the scalar finite-element formulation of a Helmholtz equation [10] in two dimensions. To the best of our knowledge, it has neither been applied to three-dimensional (3-D) EM problems, nor used with vector finite-element formulations.

Moreover, the conventional AWE method chooses the expansion point on the real frequency axis. It is known that the convergence radius of a Taylor expansion is equal to the distance from the expansion point to the nearest singu-

Manuscript received May 26, 1997; revised May 17, 1998. This work was supported by Ansoft Corporation.

The authors are with the Electrical and Computer Engineering Department, Worcester Polytechnic Institute, Worcester, MA 01609 USA.

Publisher Item Identifier S 0018-9480(98)08214-3.

larity (pole). By using only the power series expansion for the transfer function, this typically results in a very small convergence radius. One fact exploited by the AWE method is that the solution is analytic at the expansion point, and the partial realization, being a Padé approximation, is able to approximate pole behaviors much better than the power series. Nonetheless, when the expansion point is very close to a pole, the calculation of the moments will become increasingly inaccurate. Consequently, the Padé approximation will be polluted due to this inaccuracy of the moment computations, as well as the ill-conditioned matrix that is used to compute the Padé coefficients. To overcome this difficulty, various approaches such as the multipoint Padé approximation, CFH scheme, and rational Lanczos algorithm are proposed in the literature. They avoid extracting information from remote poles by catching multiple poles at multiple points.

In this paper, we apply the standard AWE method to the TVFEM analysis of passive microwave devices. Moreover, we investigate the effect of choosing a complex frequency to be the expansion center on the convergence radius in the AWE process. This choice is equivalent to deliberately slowing down the convergence in the Lanczos algorithm and subsequently reducing the pollution due to dominant modes. Through various examples, we find that the complex frequency shift can significantly enlarge the convergence range and usually provide accurate spectral responses even with a single expansion point. Additionally, in the AWE process, the most time-consuming part is to solve the matrix equations for moment matching. Although a direct method is usually the preferred choice for small or modest size problems, it is not practical for large problems. Therefore, we have employed the preconditioned conjugate gradient (PCG) method with a simple projection to both speed up and terminate the calculation of moments.

The remainder of this paper is organized as follows. In Section II, the AWE formulation for TVFEM simulation is derived. Section III describes the system singularity analysis and its relation to convergence radius. To illustrate the efficiency and accuracy of the proposed approach, Section IV presents numerical results for several microwave passive components. Finally, a brief conclusion is presented in Section V.

II. Formulation

A. Interpolation of System Equation

In the TVFEM formulation for EM boundary value problems, we choose a finite-dimensional vector subspace to be both the trial and test function space, and apply Galerkin's method to the bilinear form [1]. This process yields a matrix equation of the form

$$Ax = y \tag{1}$$

where A is a complex symmetric matrix, x is a vector whose entries represent the solution of unknown field, and y is an excitation vector. A, x, and y are implicit functions of frequency, and have dimension of $n \gg 1$. Equation (1) is typically solved for the unknown vector x at a set of discrete frequencies using either a direct method or an iterative matrix solver. As functions of frequency, A, x, and y can be assembled through the FEM for each specified frequency. For an efficient spectral-response evaluation, we need to express A and y as explicit functions of frequency. One straightforward way is to construct them through a polynomial interpolation, i.e., to expand A and y as

$$A(g) = \sum_{i=0}^{m} A_i g^i \tag{2}$$

$$y(g) = \sum_{j=0}^{n} y_j g^j \tag{3}$$

where $g = 2\times(f - f_0)/(f_h - f_l)$ is the normalized frequency, and f_0 is the central frequency. This normalization maps the frequency band $[f_l, f_h]$ onto interval $[-1, +1]$, where f_l, f_h are the lowest and highest frequencies of interest, respectively.

The orders of polynomials in (2) and (3) should be determined by the characteristics of the real problem. In our system, the underlying functions are nearly quadratic, so we choose $n = m = 3$. To minimize the numerical error and obtain stable interpolation, we choose Chebyshev nodes as the sampling points.

B. Moment Matching

Like A and y, solution x is also a function of frequency and is approximated by

$$x(g) = \sum_{i=0}^{m} x_i g^i. \tag{4}$$

Substituting (2)–(4) into (1), and matching the coefficients corresponding to the terms of the same order, we end up with the following system of linear equations:

$$\begin{aligned}
A_0x_0 &= y_0 \\
A_0x_1 + A_1x_0 &= y_1 \\
A_0x_2 + A_2x_1 + A_2x_0 &= y_2 \\
A_0x_3 + A_1x_2 + A_2x_1 + A_3x_0 &= y_3 \\
A_0x_4 + A_1x_3 + A_2x_2 + A_3x_1 &= 0 \\
&\vdots \\
A_0x_m + A_1x_{m-1} + A_2x_{m-2} + A_3x_{m-3} &= 0.
\end{aligned} \tag{5}$$

Subsequently, the power series coefficients of the solution, or the moments, can be obtained recursively by

$$\begin{aligned}
x_0 &= A_0^{-1}y_0 \\
x_1 &= A_0^{-1}(y_1 - A_1x_0) \\
x_2 &= A_0^{-1}(y_2 - A_1x_1 - A_2x_0) \\
x_3 &= A_0^{-1}(y_3 - A_1x_3 - A_2x_2 - A_3x_1) \\
x_4 &= A_0^{-1}(-A_1x_3 - A_2x_2 - A_3x_1) \\
&\vdots \\
x_m &= A_0^{-1}(-A_1x_{m-1} - A_2x_{m-2} - A_3x_{m-3}).
\end{aligned} \tag{6}$$

In modeling passive microwave components, we are usually most interested in the S-parameters. In the TVFEM formulation, for example, the S_{11} can be obtained by

$$S_{11}(g) = y^H \cdot x = \sum_{i=0}^{m} s_i g^i \tag{7}$$

where superscript H stands for Hermitian, and s_i is the ith moment of S_{11}. The number of moments m is adaptively determined by the convergence behavior of the expansion, and ultimately depends on the complexity of the system.

C. Padé Approximation

It is known that the power series of (4) or (7) always has, unfortunately, a finite radius of convergence in the presence of poles. The Padé approximation is able to approximate the function beyond the convergent region of its power series. After obtaining (7), we will force it to agree with a Padé approximate of S_{11}. The idea of Padé approximation is to replace the polynomial with a rational polynomial, which is good at catching poles. The process is letting

$$\sum_{i=0}^{m} s_i g^i = \frac{\sum_{j=0}^{p} c_j g^j}{1 + \sum_{k=1}^{q} d_k g^k} \tag{8}$$

where $p + q = m$. A different combination of p and q will produce the Padé table, and we always choose $q = p$ or $q = p + 1$. This Padé approximation is a partial realization of the original system. The details of computing the Padé coefficients can be found in [6].

D. Linear Dependence of Moments and Accelerating

In the moment calculation process when the expansion point is very close to a pole, the higher moments are usually close to linearly dependent. This can be understood easily from (6). Since the moments are computed recursively through an "inverse-power"-like method, the dominant mode of the system will eventually overshadow the other remote eigenvectors. From then on, we will not be able to acquire any significant new information from moments. This is the main drawback of the explicit moment-matching AWE method, and is also the reason why multipoint Padé form, rational Lanczos, and CFH are needed. Nonetheless, by checking the degree of linear dependence among current moments, we can determine the convergence of the dominant eigenvectors. Another benefit is that the projection of new right-hand side on the moment space is a very good initial guess for the PCG solver.

Let $x_{n+1}^{\text{app}} = \Sigma_{i=0}^{n} v_i x_i$, which is the projection of the $n+1$ moment onto the span of previous moments and $x_0, x_1, \cdots, x_n$ are previously computed moments. We then write

$$A_0 x_{n+1}^{\text{app}} = \sum_{i=0}^{n} v_i A_0 x_n. \tag{9}$$

By projecting to previous moments, we are able to determine when to terminate the moment calculation—when no significant new information is to be acquired, and to speed up the convergence in the iterative solver for higher moments.

Solving the projection of $A_0 x_{n+1}^{\text{app}} = y_{n+1}$ on the current moment space (by Galerkin's method with $\{x_0^T, x_1^T, \cdots, x_n^T\}$ as the testing space) results in

$$\sum_{i=0}^{n} v_i (x_j^T A_0 x_i) = x_j^T y_{n+1}, \qquad j = 0 \cdots n. \tag{10}$$

Once the projection x_{n+1}^{app} is obtained, we can easily check the significance of the $n+1$ moment by comparing $\|y_{n+1}^{\text{res}}\|$ to $\|y_{n+1}\|$, where $y_{n+1}^{\text{res}} = y_{n+1} - A_0 x_{n+1}^{\text{app}}$. Furthermore, the correction of $n+1$ moment satisfies $A_0 x_{n+1}^{c} = y_{n+1}^{\text{res}}$, where $x_{n+1}^{c} = x_{n+1} - x_{n+1}^{\text{app}}$. It will be shown later through various numerical examples that this projection process significantly reduces the number of iterations for computing higher moments.

III. Poles and Frequency Shift

A. Convergence Radius

The moment matching performed in (4) and (7), corresponds to a power series expansion of (1) about $g = 0.0$, i.e.,

$$x(g) = \frac{1}{A_0 + A_1 g + A_2 g^2 + A_3 g^3} y(g). \tag{11}$$

For a nonsingular A_0, we can always approximate [around $g_0 = (0, 0)$] this rational polynomial by a polynomial. That is the basis for moment matching performed above. The convergence radius of this power series is closely related to the singularities of the underlying system. More specifically, this power series is convergent only in its analytic domain with a radius equal to the distance from g_0 to the nearest pole. Although Padé approximation is known to be appropriate to approximate a function outside the analytic domain of the power series, its accuracy depends on the information from the power series (i.e., the moments) and is ultimately limited by the singularities. An analysis of these singularities will give more insight into the approximations and shed light on a better expansion point.

Since the S-parameters act as the transfer functions of the system, our focus is (8). A pole is a root of the denominator of the transfer function, i.e., a frequency at which $1 + \Sigma_{k=1}^{q} d_k g^k = 0$. We can also see that the poles are the frequencies that make the matrix $A(g)$ singular. Fig. 1 shows the pole locations in the normalized frequency plane for a microstrip patch antenna problem. We show only the poles inside the unit circle. There are five poles for this problem, and their locations are listed in Table I. We know that if a function is analytic at a point in the complex plane, then its Taylor expansion is convergent in the vicinity of that point with the convergence radius being the distance to the nearest singularity. An important observation is that all the poles are in the upper half frequency plane. That is always true for a passive system, and will be the basis for choosing a better expansion point.

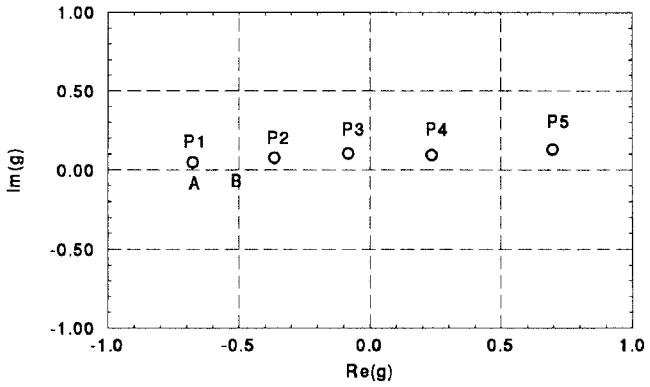

Fig. 1. Pole locations of a patch antenna problem. There are five poles in the unit circle.

TABLE I

Pole #1	(-0.676, 0.048)
Pole #2	(-0.364, 0.078)
Pole #3	(-0.082, 0.104)
Pole #4	(0.236, 0.094)
Pole #5	(0.696, 0.130)

TABLE II

Expansion Point	Convergence Radius	Distance to Nearest Pole	Valid Region on Real Axis	Valid Frequency Range
(0.0, 0.0)	0.13	0.13	[-0.13, +0.13]	2.0GHz
(0.0, -0.5)	0.61	0.61	[-0.35, +0.35]	5.6GHz

B. Frequency Shift

We have seen that poles play a critical role in determining the valid region of moment matching. By choosing a better expansion frequency, we can enlarge the convergence radius significantly. For example, in Fig. 1, a Taylor expansion at position $B(-0.514, 0.0)$ has a much larger convergence radius than that at point $A(-0.676, 0.0)$. However, even assuming that we know the exact pole locations *a priori*, it is still impossible to enlarge the convergence region much further if the expanding point is confined to the real axis. However, if we pick the expansion point from the entire complex frequency plane, we are able to keep these poles relatively far away from the expansion point, and that means a larger convergence radius. For instance, we can perform the expansion at (0.0, -0.5) instead of (0.0, 0.0). This selection does not assume knowledge of exact pole locations, and what it is based upon is just the fact that poles for a passive system can only appear in the upper half-plane. This shift provides the avenue for matching more poles at a single point. The comparison of the results is shown in Table II.

From Table II, we see that by shifting the expanding point from (0.0, 0.0) to (0.0, -0.5), the valid region of the moments has been enlarged significantly. Through shifting the expansion point to a position relatively far away from any poles, we have slowed down the convergence rate of the dominant modes and, therefore, make it possible to extract more information from moment matching at a single expansion point.

C. An Adaptive Scheme

In the implementation of the AWE algorithm, we need to adaptively determine the number of moments used for the final approximation. The convergence of the AWE can be determined through monitoring the linear dependence among the matched moments. The scheme is as follows. From (10), we have an approximation of the next moment x_{n+1}, i.e.,

$$x_{n+1}^{\text{app}} = \sum_{i=0}^{n} v_i x_i.$$

We check how close this guess is to the final solution by evaluating

$$\varepsilon = \frac{\|y_{n+1} - A_0 x_{n+1}^{\text{app}}\|}{\|y_{n+1}\|} \tag{12}$$

and, if $\varepsilon \leq \varepsilon_0$, where ε_0 is the resolution specified for PCG, then the process should stop immediately. The moments have become almost linearly dependent and a new moment can add little new information. In the following examples, we choose $\varepsilon_0 = 10^{-6}$. On the other hand, when there is no pole located within the unit circle, the magnitude of the moments will decrease monotonically, and the process can terminate when the new moment is only a small fraction of the first moment, say, 10^{-1}–10^{-2}. Thus, the number of moments can be adaptively determined by the complexity of the underlying system.

IV. Numerical Results

We have applied the algorithm described above to several practical problems to demonstrate its ability to evaluate the spectral responses in the desired frequency band. In all examples, we set $\varepsilon_0 = 10^{-6}$, and for cases when there is no pole within the unit circle, the process will be terminated when $\|x_{n+1}\|/\|x_0\| \leq 5 \times 10^{-2}$. For all the examples shown in this section, we have used the proposed procedure expanding at a single frequency point. As can be seen from the results, for some cases, we still have noticeable errors at the two ends of the spectrum. This suggests that for reliable and accurate spectral responses, the proposed approach needs to be combined with CFH-like techniques to cover wide-band operations.

A. Dielectric Waveguide with Obstacle Inside

We first consider a rectangular waveguide with a dielectric obstacle inserted inside. The geometry of the example is shown in Fig. 2. This is a simple example since there is no pole located inside the unit circle. The process stops at 20 moments with $\|x_{20}\|/\|x_0\| = 4.2 \times 10^{-2}$. The matrix dimension for the formulation is 33 720, and S_{11} is shown in Fig. 3.

B. Mitered Bend

A mitered 90° E- and H-plane waveguide bend is shown in Fig. 4. The matrix dimension is 25 428, and the reflection coefficient is shown in Fig. 5. This is also a simple problem since there is no pole within the unit circle. We simply choose the center frequency as the expansion point without any shifting. The number of moments and iterations are

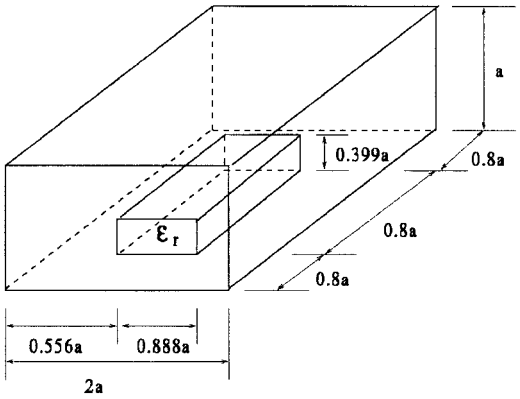

Fig. 2. Physical geometry of a waveguide with dielectric obstacle inside. $a = 1.0$ m and $\varepsilon_r = 6.0$ are used in the numerical analysis.

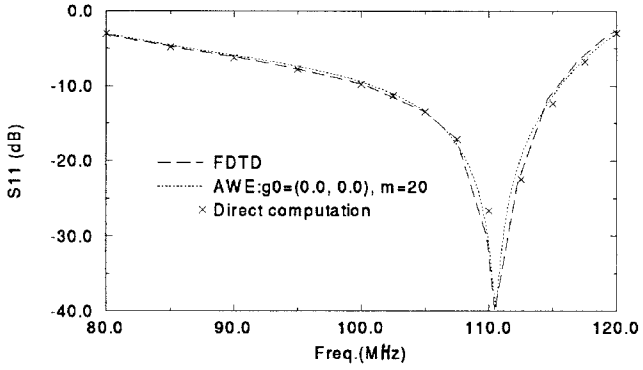

Fig. 3. The S_{11} from the current approach compared with the finite-difference time-domain's (FDTD) result and that from direct computation.

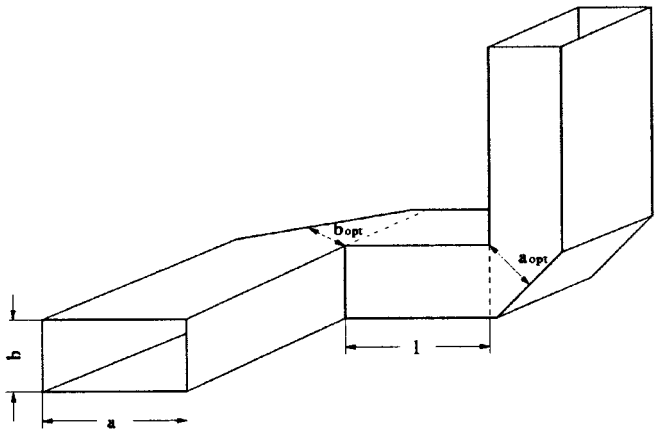

Fig. 4. The geometry of the mitered bend. $a = 22.86$ mm, $b = 10.16$ mm, $1 = b$, $a_{\rm opt} = 0.976a$, $b_{\rm opt} = 0.874b$.

shown in Fig. 6. The process terminates at 27 moments with $||x_{27}||/||x_0|| = 4.9 \times 10^{-2}$.

C. Microstrip Low-Pass Filter

Another example that we considered here is a microstrip low-pass filter with its geometry, shown in Fig. 7. The system has pole(s) in the unit circle since the moments have a convergence radius smaller than one. If expansion is performed at $g_0 = (0.0, 0.0)$, the power series will have a convergence radius of 0.26 if the expansion point is shifted to (0.0, -0.5) and then convergence radius becomes 0.68. On the real frequency axis, this corresponds to a convergent interval (-0.46, $+0.46$). The matrix dimension is 29 592 and the S_{11} parameters produced by these two expansions are shown in Fig. 8, with the PCG performances for solving the moments

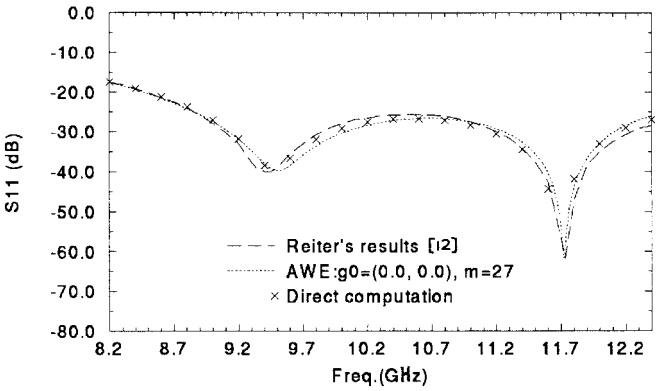

Fig. 5. The S_{11}-parameter from the current approach. Results from literature and direct calculation are also shown.

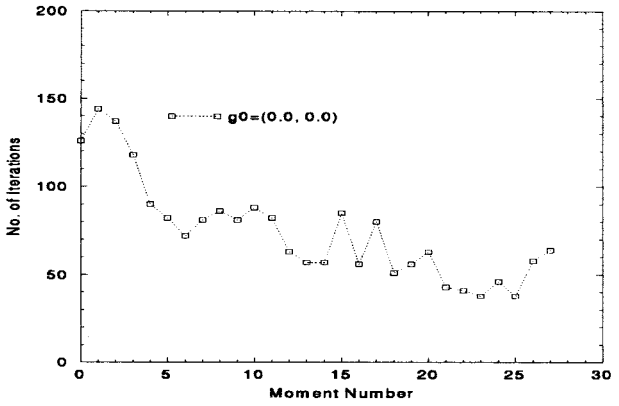

Fig. 6. Moment convergence via number of moments. The process stops at 28 moments.

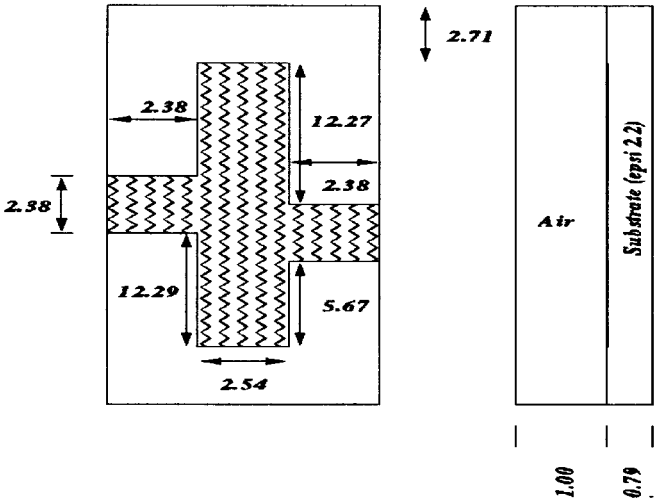

Fig. 7. The physical geometry of a microstrip low-pass filter with $\varepsilon_r = 2.2$. Top view dimensions in millimeters.

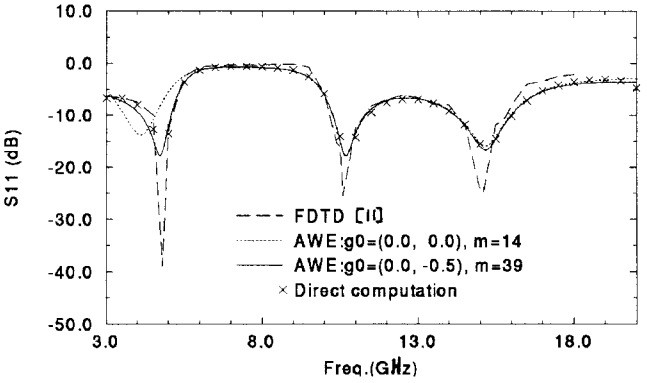

Fig. 8. S_{11} of this low-pass filter for expansions at origin and a shift point. The former terminates at 14 moments, while the shift case goes to 39 moments.

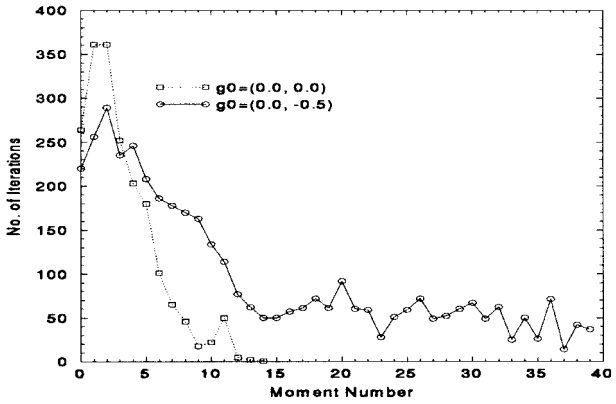

Fig. 9. Convergence behaviors of shift and unshift cases.

shown in Fig. 9. As can be seen from the figure, the number of iterations decreases significantly for higher moments.

Although the expansion at (0.0, 0.0) can nearly give the correct results, an expansion at (0.0, −0.5) can do even better. For the (0.0, 0.0) case, the expansion stopped at $m = 14$. The expansion at (0.0, −0.5) converges at a slower rate, and the process continues until $m = 39$. Thus, by shifting from (0.0, 0.0) to (0.0, −0.5), we have slowed down the convergence of the dominant eigenvectors and, subsequently, extract more information from a single-point moment matching.

D. Microstrip Patch Antenna

The last example considered here is a microstrip patch antenna (see Fig. 10). The matrix dimension of the FEM formulation is 33 758 with 641K total nonzero entries. The poles have been shown in Fig. 1, and the convergence behavior has been analyzed in Section III. The reflection coefficient shown in Fig. 11 for g_0 is chosen to be (0.0, 0.0) and (0.0, −0.5) and is compared with FDTD results. The number of total moments and the iteration number for the PCG solver for each moment are shown in Fig. 12.

For the $g_0 = (0.0, 0.0)$ case, the dominant eigenvectors converge too fast, and after 12 moments, there is virtually no new information contained in the subsequent moments. Consequently, the approximation cannot get enough information to estimate the solution beyond the 8.0- and 17.5-GHz interval. A better result was obtained by shifting the expansion point to

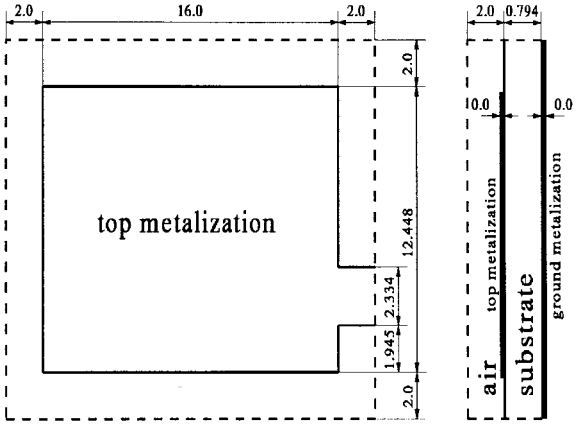

Fig. 10. Top and side views of a microstrip patch antenna.

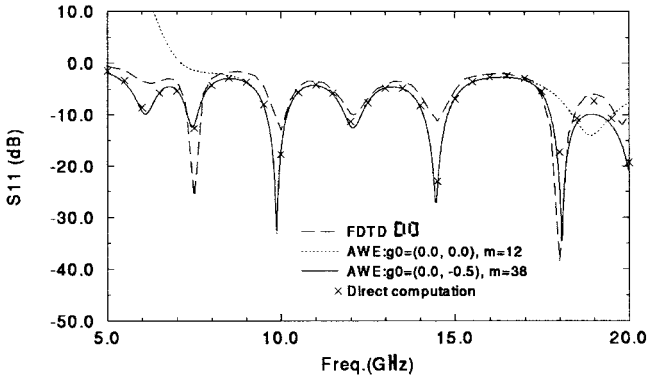

Fig. 11. S_{11} from two expansions, compared with the FDTD's result and direct computation.

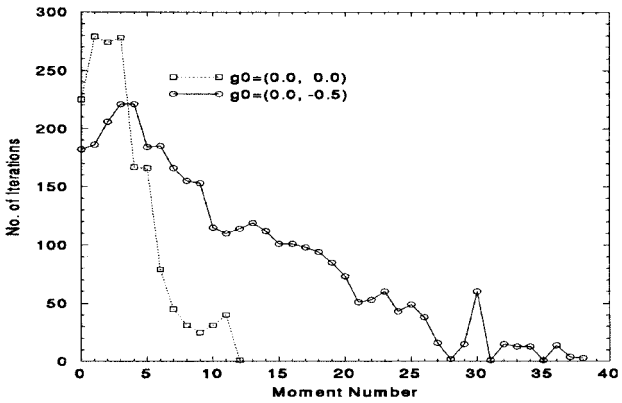

Fig. 12. Convergence of moment matching for $g_0 = (0.0, 0.0)$ and $g_0 = (0, 0, -0.5)$.

(0.0, −0.5). This time, the process goes to 38 moments, and gives better results for the entire frequency band.

V. Conclusions

The application of the AWE method to TVFEM simulation of microwave devices has been presented in this paper. The combination of a PCG iterative solver and the frequency shift yields a very efficient AWE-based fast frequency-sweep technique. Since the iterative method was employed to match moments, the size of the problem could be large. Also, due

to the iterative solver, the algorithm is ready to incorporate a frequency-hopping technique.

REFERENCES

[1] J. F. Lee, D. K. Sun, and Z. J. Cendes, "Full-wave analysis of dielectric waveguides using tangential vector finite elements," *IEEE Trans. Microwave Theory Tech.*, vol. 39, pp. 1262–1271, Nov. 1991.

[2] J. F. Lee, G. M. Wilkins, and R. Mittra, "Finite-element analysis of axisymmetric cavity resonator using a hybrid edge element technique," *IEEE Trans. Microwave Theory Tech.*, vol. 41, pp. 1981–1987, Nov. 1993.

[3] L. T. Pillage and R. A. Rohrer, "Asymptotic waveform evaluation for timing analysis," *IEEE Trans. Computer-Aided Design*, vol. 9, pp. 352–366, Apr. 1990.

[4] S. Kumashiro, R. A. Rohrer, and A. J. Strojwas, "Asymptotic waveform evaluation for transient analysis of 3-D interconnect structures," *IEEE Trans. Computer-Aided Design*, vol. 12, pp. 988–996, July 1993.

[5] K. Gallian, E. Grimme, and P. Van Dooren, "Asymptotic waveform evaluation via a Lanczos method," *Appl. Math. Lett.*, vol. 7, pp. 75–80, 1994.

[6] X. Yuan and Z. J. Cendes, "A fast method for computing the spectral response of electromagnetic circuits," presented at the APS/URSI Meeting, Ann Arbor, MI, 1993.

[7] E. J. Grimme, D.C. Sorensen, and P. Van Dooren, "Model reduction of state space systems via an implicitly restarted," *Numer. Algorithms*, vol. 12, pp. 1–32, Apr. 1996.

[8] K. Gallian, E. Grimme, and P. Van Dooren, "A rational Lanczos algorithm for model reduction," *Numer. Algorithms*, vol. 12, pp. 33–64, Apr. 1996.

[9] E. Chiprout and M. S. Nakhla, "Analysis of interconnect networks using complex frequency hopping (CFH)," *IEEE Trans. Computer-Aided Design*, vol. 14, pp. 186–200, Feb. 1995.

[10] M. A. Kolbehdari, M. Srinivasan, M. S. Nakhla, Q. J. Zhang, and R. Achar, "Simultaneous time and frequency domain solutions of EM problems using finite element and CFH techniques," *IEEE Trans. Microwave Theory Tech.*, vol. 44, pp. 1562–1534, Sept. 1996.

[11] D. M. Sheen, S. M. Ali, M. D. Abouzahra, and J. A. Kong, "Application of the three-dimensional finite-difference time-domain method to the analysis of planar microstrip circuits," *IEEE Trans. Microwave Theory Tech.*, vol. 38, pp. 849–857, July 1990.

[12] J. M. Reiter and F. Arndt, "Rigorous analysis of arbitrary shaped H- and E-plane discontinuities in rectangular waveguides by a full-wave boundary contour mode-matching method," *IEEE Trans. Microwave Theory Tech.*, vol. 43, pp. 796–801, Apr. 1995.

Xiao-Ming Zhang, photograph and biography not available at the time of publication.

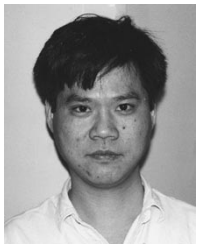

Jin-Fa Lee (M'88) was born in Taipei, Taiwan, R.O.C., in 1960. He received the B.S. degree from the National Taiwan University, Taipei, Taiwan, R.O.C., in 1982, and the M.S. and Ph.D. degrees from Carnegie-Mellon University, Pittsburgh, PA, in 1986 and 1989, respectively, all in electrical engineering.

From 1988 to 1990, he was with the Ansoft Corporation, Pittsburgh, PA, where he developed several computer-aided design finite-element programs for modeling 3-D microwave and millimeter-wave circuits. From 1990 to 1991, he was a Post-Doctoral Fellow at the University of Illinois at Urbana-Champaign. He is currently an Associate Professor in the Department of Electrical and Computer Engineering, Worcester Polytechnic Institute, Worcester, MA. His current research interests are analyses of numerical methods, fast matrix-solution techniques, 3-D mesh generation, h- and hp-versions of adaptive mesh refinement in FEM's, designs of RF/microwave circuits and antennas, and nonlinear optic-fiber modelings.